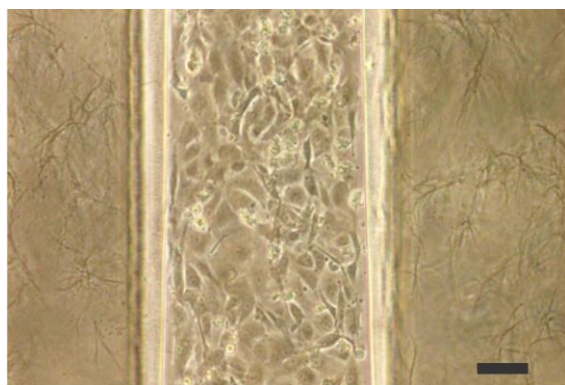


Electronic Supplementary Information

1. Movie S1 A time sequence of images of the MBA-MD-231 cells embedded in collagen in the absence (left side) and presence (right side) of the flow (3.5 $\mu\text{m}/\text{sec}$). The size of each image is 400 μm x 552 μm . The movie was taken at $t = 14$ hours, the time between the two consecutive images is 5 min, and the movie has 25 frames.

2. Figure S1 A phase contrast microscopy image of a confluent HUVECs monolayer between two collagen filled channels. Scale bar: 100 μm .



3. Numerical simulation of interstitial and intramural flow profiles

Computation of interstitial flow COMSOL Multiphysics 4.3 was used to compute the flow field within the collagen matrix. The computation setting was taken from Figure 2 (A,C), where the fluid flow comes in from the flow channel, through the collagen matrix and exit through the other side of the flow channel. Here, collagen was introduced into all three cell channels (note the difference to Figure 2C where only one channel is filled), and the pressure at the exit of the flow channel is $P = 0$. For flow field in the region without collagen, we used Navier-Stokes equation. For flow fields within collagen, we solved the steady state Brinkman Equation for a porous medium (Polacheck et al. PNAS, 2011):

$$\mu \nabla^2 \vec{u} - \frac{\mu}{\kappa} \vec{u} = \vec{\nabla} P,$$

where \vec{u} is the interstitial flow speed, μ is the fluid's dynamic viscosity, and κ is the permeability of the porous media. No-slip boundary conditions are given for all other boundaries, including the top, bottom, and side walls for all flow and cell channels, and the surfaces of the microfabricated contact lines. The permeability κ of the 0.15% type I collagen is 10^{-11} m^2 (Cross et al, Biomaterials, 2010), and the water dynamic viscosity $\mu = 0.000855 \text{ Pa}\cdot\text{s}$. The resultant flow fields are shown in Figure 4G-H.

Computation of both intramural and interstitial flows within the same microfluidic platform We used Brinkman Equation and Navier-Stokes Equation to simulate the pressure field distribution and flow fields for generating both interstitial and intramural flow at the same time. The computation setting was taken from Figure 2B with the collagen gel in two side cell channels. Intramural flow was introduced through the center cell channel, while interstitial flow was introduced from the flow channel. Specific pressures are provided as boundary conditions, as shown in Figure S1. These pressures are chosen to generate a interstitial flow of a few micrometers per second, and an average intramural flow of ~ 50 micrometer per second.

Figure S2 shows that the maximum flow speed in the center intramural channel is roughly $50 \mu\text{m}/\text{sec}$, and the speed of interstitial flow in the collagen is $6\text{-}7 \mu\text{m}/\text{sec}$. The black solid lines are the streamlines, showing the flow direction. The interstitial flows are spatially uniformly distributed leftward, and the intramural flow is mostly downward.

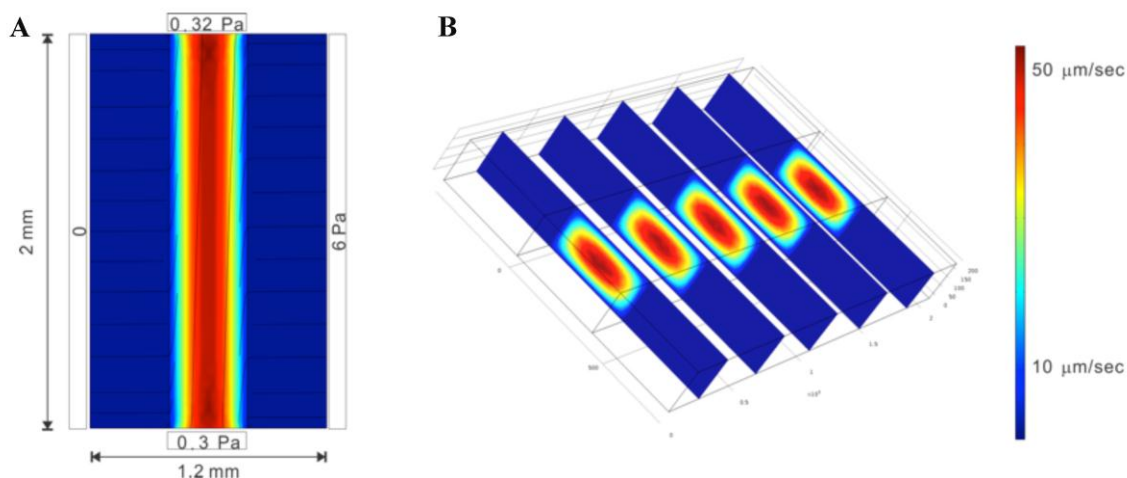


Figure S2: Computed interstitial and intramural flow fields A: Colored rendition of the flow speed profiles for the setting where the two side channels are filled with collagen (blue channels) and center channel with media (red channel). The pressure heads are given as boundary conditions, where the inlet of the central intramural flow channel is 0.32 Pas and outlet 0.3 Pas., inlet of the interstitial flow channel is 6 Pas and outlet 0. A uniform interstitial flow ($6\text{-}7 \mu\text{m}/\text{sec}$) is generated within the two side channels and a Poiseuille intramural flow (maximum speed of $50 \mu\text{m}/\text{sec}$) is generated in the center channel. The black solid lines mark the streamlines, which are horizontal within the collagen, and mostly vertical within the vessel. B: 3D rendition of the same flow fields. Length is shown in μm .

4. Cell migration data analysis

We provide here additional data to support the claim in the main text that motility of a sub-population of cells (aspect ratio between 1-2) was enhanced by the presence of the flow.

Exp 1	Control		Flow				
Aspect ratio	Variance ($\mu\text{m/s}$)	# of points	Variance ($\mu\text{m/s}$)	# of points	F-value	p-value	
1.0-2.0	5.49734	606	9.115607	800	1.658185	0	****
2.0-3.0	7.824829	186	9.608927	98	1.228005	0.11774014	
3.0-4.0	11.43965	97	8.847735	57	1.292947	0.14857807	
4.0-5.0	6.604021	68	7.737844	34	1.171687	0.28682026	
5.0-6.0	4.77068	40	10.07384	26	2.111615	0.01760323	*
Exp 2	Control		Flow				
Aspect ratio	Variance ($\mu\text{m/s}$)	# of points	Variance ($\mu\text{m/s}$)	# of points	F-value	p-value	
1.0-2.0	5.069954	475	7.33907	606	1.447561	0.00001248	****
2.0-3.0	5.200225	145	7.570855	151	1.455871	0.01184776	**
3.0-4.0	5.133333	104	9.424974	73	1.836034	0.00191436	*
4.0-5.0	5.777233	76	9.418357	45	1.630254	0.03104658	*
5.0-6.0	4.828071	37	4.801579	26	1.005517	0.4513812	
Exp 3	Control		Flow				
Aspect ratio	Variance ($\mu\text{m/s}$)	# of points	Variance ($\mu\text{m/s}$)	# of points	F-value	p-value	
1.0-2.0	9.944122	373	11.69652	485	1.176225	0.04921741	*
2.0-3.0	15.81855	150	16.16372	182	1.021821	0.4472308	
3.0-4.0	16.83721	88	15.13892	115	1.11218	0.29565245	
4.0-5.0	13.44612	74	11.64465	54	1.154704	0.29271726	
5.0-6.0	13.74011	48	16.05896	38	1.168765	0.30418703	

Table S1: Variances of V_x for cells of various sub-groups defined by the range of the cell aspect ratio. The p-value is obtained using the standard t-test analysis.